Stem Cell Reports
Report

ISSCR

OPEN ACCESS

Inhibition of CDK5 Alleviates the Cardiac Phenotypes in Timothy Syndrome

LouJin Song,[1,2,3] Seon-hye E. Park,[1,2,5] Yehuda Isseroff,[1,2,4] Kumi Morikawa,[1,2] and Masayuki Yazawa[1,2,3,*]
[1]Columbia Stem Cell Initiative, Columbia University, New York, NY 10032, USA
[2]Department of Rehabilitation and Regenerative Medicine, Columbia University, New York, NY 10032, USA
[3]Department of Pharmacology, Columbia University, New York, NY 10032, USA
[4]College of Dental Medicine, Columbia University, New York, NY 10032, USA
[5]Present address: The Graduate School of Biomedical Sciences, The University of Texas Southwestern Medical Center, Dallas, TX 75390, USA
*Correspondence: my2387@cumc.columbia.edu
http://dx.doi.org/10.1016/j.stemcr.2017.05.028

SUMMARY

L-type calcium channel $Ca_V1.2$ plays an essential role in cardiac function. The gain-of-function mutations in $Ca_V1.2$ have been reported to be associated with Timothy syndrome, a disease characterized by QT prolongation and syndactyly. Previously we demonstrated that roscovitine, a cyclin-dependent kinase (CDK) inhibitor, could rescue the phenotypes in induced pluripotent stem cell-derived cardiomyocytes from Timothy syndrome patients. However, exactly how roscovitine rescued the phenotypes remained unclear. Here we report a mechanism potentially underlying the therapeutic effects of roscovitine on Timothy syndrome cardiomyocytes. Our results using roscovitine analogs and CDK inhibitors and constructs demonstrated that roscovitine exhibits its therapeutic effects in part by inhibiting CDK5. The outcomes of this study allowed us to identify a molecular mechanism whereby $Ca_V1.2$ channels are regulated by CDK5. This study provides insights into the regulation of cardiac calcium channels and the development of future therapeutics for Timothy syndrome patients.

INTRODUCTION

L-type calcium channel $Ca_V1.2$ plays an essential role in cardiac development and function (Flucher and Franzini-Armstrong, 1996; Seisenberger et al., 2000). The missense mutations in *CACNA1C* encoding $Ca_V1.2$ channel are associated with Timothy syndrome (TS), a multisystem disorder that features long-QT syndrome and syndactyly (Boczek et al., 2015; Hennessey et al., 2014; Papineau and Wilson, 2014; Splawski et al., 2004). TS patients are treated clinically with β-adrenergic blockers, calcium channel blockers, and sodium channel blockers (Jacobs et al., 2006; Shah et al., 2012). However, these regimens are insufficient to prevent lethal arrhythmias in TS patients (Corona-Rivera et al., 2015; Kawaida et al., 2016; Philipp and Rodriguez, 2016). Therefore, new therapeutics for TS are still needed. Previously, we found that roscovitine, a cyclin-dependent kinase (CDK) inhibitor, could rescue the phenotypes in human induced pluripotent stem cell (iPSC)-derived cardiomyocytes (CMs) and neurons from TS patients (Pasca et al., 2011; Song et al., 2015; Yazawa et al., 2011). However, the mechanisms whereby roscovitine restores the cardiac functions in TS CMs have not been fully elucidated. In this study, we sought to investigate the mechanisms underlying the beneficial effects of roscovitine on TS CMs and to identify additional therapeutic compounds for TS.

RESULTS

Roscovitine Analog and CDK Inhibitor Tests

To confirm the cause of this disease and obtain ideal controls for the TS iPSCs, we generated isogenic control iPSCs from the TS iPSCs using TALEN (transcription activator-like effector nuclease) technology, and characterized the isogenic control iPSCs (Figure S1). The isogenic control iPSCs demonstrated a normal karyotype and pluripotency, and the CMs derived from the isogenic control iPSCs showed regular calcium transients in calcium imaging and normal voltage-dependent inactivation percentage values in voltage-clamp recordings, which are comparable with the values in CMs derived from non-isogenic control iPSCs generated from skin fibroblasts of healthy donors (Figures S1A–S1J). To search for roscovitine analogs that are more potent or less toxic than roscovitine and explore the mechanisms underlying the effects of roscovitine on TS CMs, we tested 20 roscovitine analogs and four CDK inhibitors with different specificities against CDKs using a contraction assay with MATLAB-based analysis (Huebsch et al., 2015; Yazawa et al., 2011) and calcium imaging (Figure 1A). Two rounds of chemical test were conducted to examine the effects of the compounds. The first round of chemical testing was conducted using TS CM clusters isolated from the monolayer CMs to screen and identify the positive compounds that could increase the spontaneous beating rate and decrease the contraction irregularity of the TS CM clusters (Figures S2A–S2C and Table S1). The subsequent test was conducted using the intact monolayer CMs to validate the beneficial effects of the positive compounds on TS CMs and to eliminate the potential bias that could be caused by isolating the CMs from the original culture (Figures 1B–1D). From the chemical tests, we identified two roscovitine analogs, CR8 and Myoseverin-B, and two CDK inhibitors, PHA-793887 and DRF053, that had beneficial effects on TS CMs

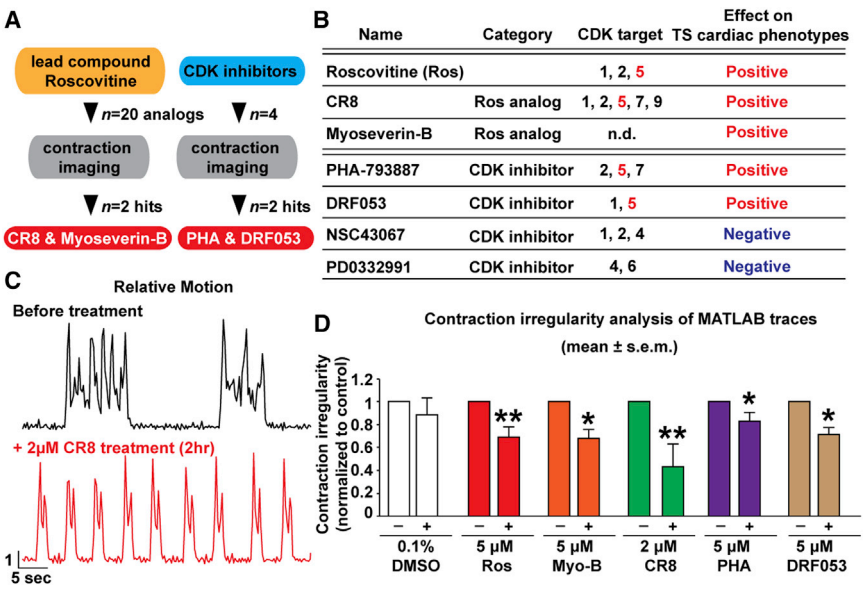

Figure 1. Summary of Roscovitine Analog and CDK Inhibitor Tests

(A) Schematic illustration of roscovitine analog and CDK inhibitor tests.

(B) A summary of the CDK targets of the positive roscovitine analogs and CDK inhibitors. Eighteen other roscovitine analogs did not show positive effects (see Table S1). n.d., CDK targets are not yet determined.

(C) Representative traces from the MATLAB-based analysis of TS CM contractions before treatment and 2 hr after the treatment of 2 μM CR8.

(D) The analysis of contraction irregularity of TS CMs before treatment and 2 hr after the treatment of each positive compound (n = 10 for the chemical compounds and n = 5 for DMSO control from one TS iPSC line; the irregularity value after treatment was normalized to the corresponding irregularity value before treatment for each sample in each group). *p < 0.05, **p < 0.01; Student's t test, paired. Ros, roscovitine; Myo-B, myoseverin-B; PHA, PHA-793887. The replicates (n) are independent biological replicates from multiple rounds of experiments. See Table S2 for detailed information about the iPSC lines used for each experiment.

(Figures 1B–1D and S2; Table S1; Movie S1). When we summarized the CDK targets of all positive compounds, it was found that four out of the five positive compounds have been reported to inhibit CDK5 (Bettayeb et al., 2008; Brasca et al., 2010; Meijer et al., 1997; Oumata et al., 2008) (Figures 1B, S2G, and S2H), suggesting that CDK5 could be involved in the molecular mechanisms underlying TS.

The Effects of CDK5 Inhibition on TS CMs

To examine whether CDK5 inhibition is beneficial for TS CMs, we first constructed a lentivirus containing the dominant negative (DN) mutant of CDK5. We used patch-clamp recordings and calcium imaging to assess the physiological properties of the TS CMs infected with the CDK5 DN lentivirus. The phenotypes of TS CMs include a delayed voltage-dependent inactivation of $Ca_V1.2$ channels, abnormal action potentials, and abnormal calcium transients (Song et al., 2015; Yazawa et al., 2011). The TS CMs with CDK5 DN expression demonstrated a significantly enhanced voltage-dependent inactivation of $Ca_V1.2$ channels compared with the CMs without CDK5 DN expression (Figures 2A–2C). Moreover, the expression of CDK5 DN significantly shortened the paced action potential duration and rescued the abnormal spontaneous action potentials in TS CMs (Figures 2D, 2E, S3A, and S3B; Table S3). In addition, we examined the effects of CDK5 DN expression on the calcium currents in TS CMs. The results suggest that TS CMs demonstrated more late calcium currents compared with control CMs, and the expression of CDK5 DN significantly reduced the late calcium currents in TS CMs (Figures S3C–S3E). Finally, CDK5 DN expression alleviated the abnormal spontaneous calcium transients and paced calcium transients, and significantly reduced the calcium transient duration and half decay time in the paced TS CMs (Figures 2F–2J and S3F–S3M). Overall, the results indicated that CDK5 DN expression could alleviate all the previously reported phenotypes in TS CMs.

Next, we examined the effect of roscovitine on the TS CMs infected with the CDK5 DN lentivirus, to investigate whether CDK5 inhibition partially accounts for the therapeutic effects of roscovitine on TS CMs. The results showed that roscovitine did not further enhance the voltage-dependent inactivation of $Ca_V1.2$ in TS CMs with CDK5 DN expression, indicating that CDK5 DN expression is sufficient to rescue the delayed voltage-dependent inactivation of $Ca_V1.2$ in TS CMs (Figures 2K and 2L).

To validate our findings using another approach, we designed short hairpin RNA (shRNA) lentiviral constructs that target CDK5 and confirmed the knockdown efficiency of the constructs (Figures S4A–S4C). We then infected TS CMs with the CDK5 shRNA lentivirus and examined the effects of CDK5 shRNA expression on the reported phenotypes in TS CMs. CDK5 shRNA expression significantly enhanced the voltage-dependent inactivation of $Ca_V1.2$ in TS CMs (Figures 2M and 2N). In addition, CDK5 shRNA expression alleviated the abnormal spontaneous calcium transients in TS CMs (Figures S3M and S4D–S4F). The effects of CDK5 shRNA expression on TS CMs were thus

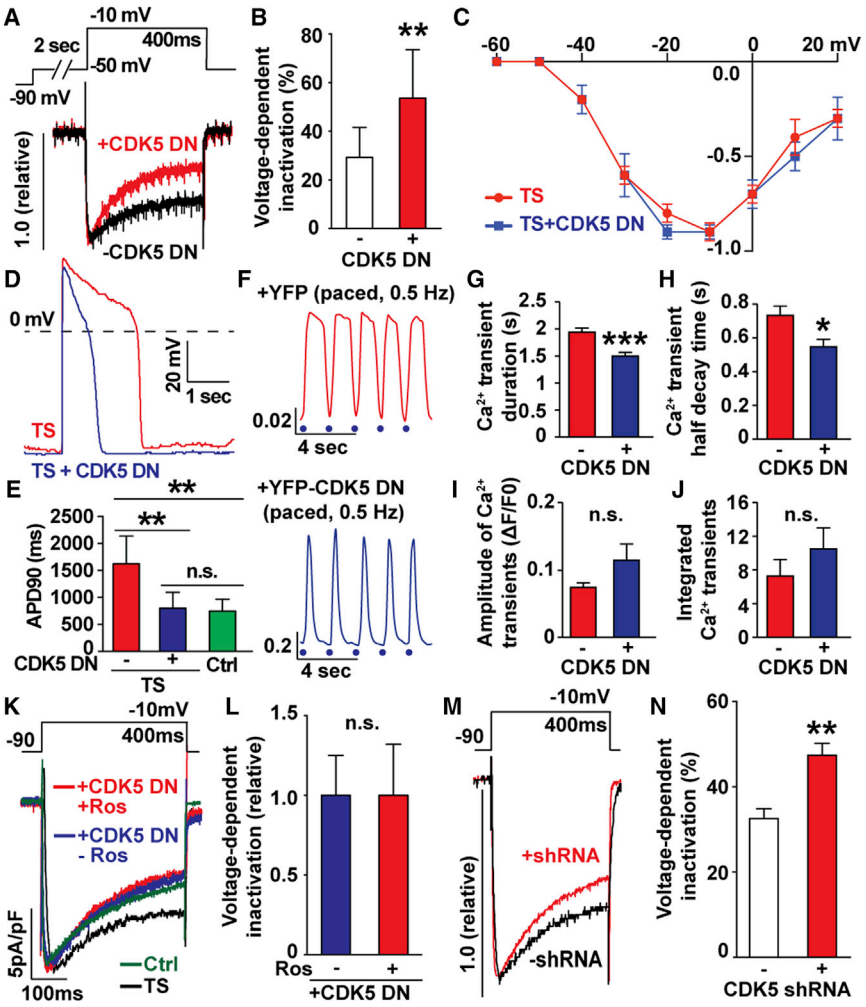

Figure 2. CDK5 Inhibition Alleviated the Phenotypes in TS CMs

(A) Representative voltage-clamp recordings of Ba^{2+} currents in the TS CM with (+CDK5 DN) and without (−CDK5 DN) CDK5 DN expression. "1.0 (relative)" means that the data points were normalized to the corresponding peak current value to make the traces.

(B) Voltage-dependent inactivation percentage quantification in TS CMs with (n = 19) and without (n = 7) CDK5 DN expression. Data are mean ± SD.

(C) The current-voltage relationships of the Ba^{2+} currents in TS CMs with (squares, n = 19) and without (circles, n = 7) CDK5 DN expression are statistically not significantly different.

(D) Representative paced (0.2 Hz) action potential recordings in the CDK5 DN lentivirus infected (+CDK5 DN) and uninfected TS CM.

(E) Action potential duration at 90% of repolarization (APD90) quantification in the control CMs (n = 10 from three lines) and the TS CMs with (n = 10 from two lines) and without (n = 8 from two lines) CDK5 DN expression (one-way ANOVA with Bonferroni post hoc).

(F) Representative Ca^{2+} transient traces of paced (0.5Hz) single TS CM infected with the R-GECO1 lentivirus and the YFP lentivirus or the YFP-CDK5 DN lentivirus. Blue dots indicate electrical pulses (2 ms, bipolar pulse, 4 V). The expression of CDK5 DN alleviated the abnormal paced Ca^{2+} transients in TS CMs. y Axis, $\Delta F/F_0$ for R-GECO1 (calcium fluorescence indicator).

(G–J) The analysis of Ca^{2+} transient duration, half decay time, amplitude, and integrated calcium transients (area under curve) in the paced TS CMs with and without CDK5 DN expression (n = 7 for the group without CDK5 DN, n = 17 for the group with CDK5 DN).

(K) Representative voltage-clamp recordings of Ba^{2+} currents in single TS CM with CDK5 DN expression before (blue) and after roscovitine treatment (red, 5 μM, 3 min).

(L) Roscovitine did not significantly enhance the voltage-dependent inactivation of $Ca_V1.2$ in TS CMs with CDK5 DN expression (n = 9). Data are mean ± SD.

(M) Representative recordings of Ba^{2+} currents in the TS CM with (+shRNA) and without (−shRNA) CDK5 shRNA expression.

(N) Voltage-dependent inactivation percentage quantification in TS CMs with (n = 13) and without (n = 9) CDK5 shRNA expression.

Data in (C), (E), (G–J), and (N) are mean ± SEM. Data were from two lines and Student's t test was used for statistics unless otherwise stated. n.s., not significant; *p < 0.05, **p < 0.01, ***p < 0.005. The replicates (n) are independent biological replicates from multiple rounds of experiments. See Table S2 for detailed information about the iPSC lines used for each experiment.

similar to the effects of CDK5 DN expression on TS CMs, indicating that CDK5 inhibition is beneficial for TS CMs.

The Molecular Mechanism Underlying the Positive Effects of CDK5-Specific Inhibition on TS CMs

The positive effects of CDK5-specific inhibition on TS CMs prompted us to investigate its underlying mechanisms. CDK5 has been reported to phosphorylate serine or threonine in two consensus sequences, S/T-P-X-R/H/K and P-X-S/T-P (where X is any amino acid) (Dhariwala and Rajadhyaksha, 2008; Plattner et al., 2014). We examined the sequences of $Ca_V1.2$ channels and found five consensus sequences located at the II-III loop and the C terminus (C-term), which are conserved in both humans and rodents

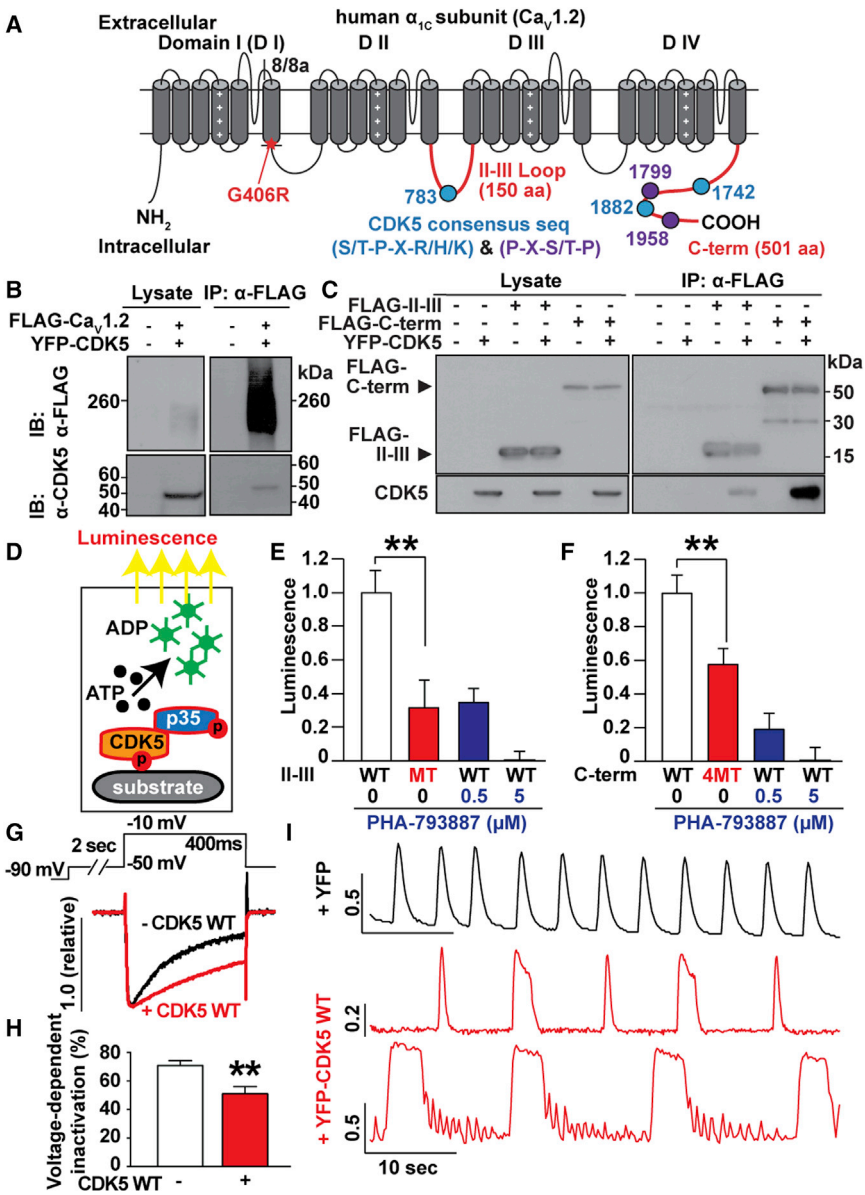

Figure 3. Direct Interaction and Phosphorylation between CDK5 and $Ca_V1.2$

(A) The structure of human $Ca_V1.2/\alpha1c$ subunit. The G406R mutation and five CDK5 consensus sequences in $Ca_V1.2$ are shown.

(B and C) Co-immunoprecipitation (IP) was performed using FLAG antibody resins with HEK 293T cell lysates expressing YFP-CDK5 and FLAG-$Ca_V1.2$ (B), or FLAG-II-III loop (C), or FLAG-carboxyl terminus (C-term, C). Anti-(α-)human CDK5 and FLAG-tag antibodies were used for immunoblotting (IB).

(D) Design of the in vitro kinase assay. The phosphorylation of the substrates by activated CDK5 consumes ATP and produces ADP that is converted into luminescence.

(E and F) Wild-type (WT) II-III loop (II-III) and C terminus (C-term) were phosphorylated by CDK5. PHA-793887 (PHA) and the mutagenesis (II-III Mutant [MT]: S783G; C-term 4MT: S1742A/S1799A/S1882A/T1958A) blocked the phosphorylation (II-III: n = 3 for both PHA groups and n = 6 for WT and MT groups; C-term: n = 6 for both PHA groups and n = 9 for WT and MT groups). **p < 0.01, Student's t test for WT versus MT/4MT; data are mean ± SEM.

(G) Representative recordings of Ba^{2+} currents in control CM with and without CDK5 WT overexpression.

(H) CDK5 WT overexpression significantly delayed the voltage-dependent inactivation of $Ca_V1.2$ in control CMs (n = 14 for −CDK5 WT group and n = 12 for +CDK5 WT group from two control lines; **p < 0.01, Student's t test; data are mean ± SEM).

(I) Representative Ca^{2+} transient traces of control CMs infected with the R-GECO1 lentivirus and the YFP lentivirus (n = 24 from two lines) or the YFP-CDK5 WT lentivirus (n = 20 from two lines). y Axis, $\Delta F/F_0$ for R-GECO1 (calcium fluorescence indicator).

The replicates (n) are independent biological replicates from multiple rounds of experiments. See Table S2 for detailed information about the iPSC lines used for each experiment.

(Figure 3A). We generated plasmids containing FLAG-tagged full-length $Ca_V1.2$ and YFP-tagged CDK5 for a co-immunoprecipitation (coIP) assay. The coIP results demonstrated a binding of CDK5 with $Ca_V1.2$ (Figure 3B). Next, we generated FLAG-tagged II-III loop and FLAG-tagged C-term of $Ca_V1.2$ constructs to repeat the coIP assay, and validated the binding of CDK5 with the two fragments (Figure 3C).

To examine whether CDK5 phosphorylates $Ca_V1.2$, we designed an in vitro kinase assay. The wild-type II-III loop or the C-term of $Ca_V1.2$ was used as the substrates in this assay. We generated mutant II-III loop and mutant C-term constructs with substitutions of serine/threonine to glycine or alanine in all CDK5 consensus sequences as negative controls (Figures S4G and S4H). The phosphorylation of the substrates by CDK5 consumes ATP and produces ADP, which is then converted into luminescence by detection reagents in the assay (Figure 3D). The luminescence signal was reduced when we added the CDK5 inhibitor, PHA-793887, to the reactions using wild-type II-III loop

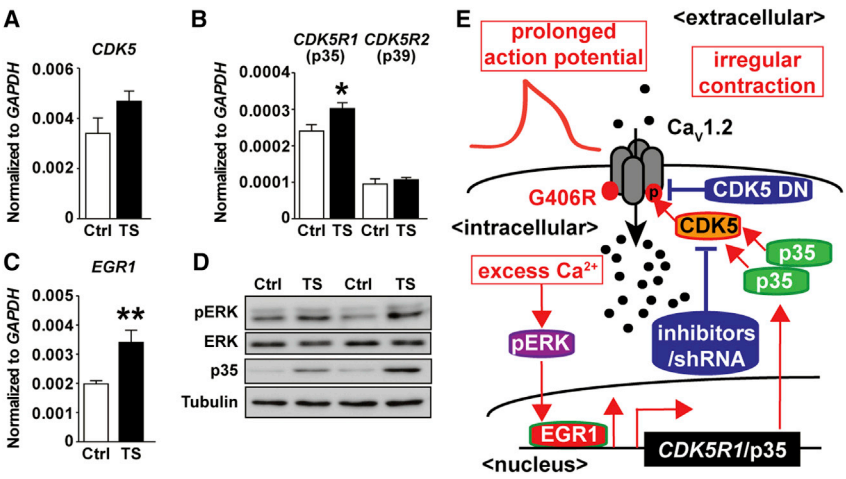

Figure 4. One of the Potential Mechanisms Underlying the Effects of CDK5 Inhibition on TS CMs

(A–C) *GAPDH* was used to normalize *CDK5*, *CDK5R1* (p35), *CDK5R2* (p39), and *EGR1* expression in the qPCR analysis (*p < 0.05, **p < 0.01; Student's t test; data are mean ± SEM). CM samples from four control lines (Ctrl, n = 12 for *CDK5*, *CDK5R1*, *CDK5R2*, and n = 9 for *EGR1* including two isogenic control lines) and two TS lines (TS, n = 14 for *CDK5*, *CDK5R1*, *CDK5R2* and n = 9 for *EGR1*) were tested.

(D) Phosphorylated ERK (pERK) and p35 proteins were increased in TS CMs compared with control (Ctrl) CMs.

(E) Schematic presentation of the proposed signaling pathway in TS CMs.

The replicates (n) for this figure are independent biological replicates from multiple rounds of experiments. See Table S2 for detailed information about the iPSC lines used for each experiment.

or C-term as the substrates. Moreover, the luminescence signal was significantly reduced when using mutant II-III loop or C-term as the substrates, compared with using wild-type II-III loop or C-term as the substrates in the kinase reactions. The results indicated the phosphorylation of the II-III loop and the C-term of Ca$_V$1.2 by CDK5 in vitro (Figures 3E and 3F). The remaining signals in the mutant II-III loop and C-term could result from the phosphorylation of p35 by CDK5 (Asada et al., 2012) and/or non-specific phosphorylation of some serine/threonine residues in the mutant II-III loop and C-term. To provide additional support for the in vitro biochemical results, we examined whether wild-type CDK5 overexpression alters Ca$_V$1.2 channel functions in control CMs. We observed that wild-type CDK5 overexpression significantly delayed the voltage-dependent inactivation of Ca$_V$1.2 (Figures 3G and 3H) and induced abnormal calcium transients in control CMs (Figure 3I). Taken together, the results demonstrated that CDK5 potentially affects Ca$_V$1.2 functions by direct binding and phosphorylation, and that CDK5 overexpression could result in delayed voltage-dependent inactivation of Ca$_V$1.2 in control CMs.

To further explore the signaling pathways underlying the effects of CDK5 inhibition on TS CMs, we measured the mRNA expression of *CDK5* and its activator p35 (*CDK5R1*) and p39 (*CDK5R2*) in control and TS CMs. We found a significant increase in the mRNA expression of p35 (*CDK5R1*) in TS CMs compared with controls (Figures 4A and 4B). We next measured the expression of EGR1, a transcription factor that regulates p35 transcription (Harada et al., 2001; Shah and Lahiri, 2014), and observed a significant increase in *EGR1* mRNA expression in TS CMs (Figure 4C). We found that the increased p35 (*CDK5R1*) mRNA expression led to an increased p35 protein expression and a hyperactivation of CDK5 in TS CMs (Figures 4D and S4I–S4K). We then examined the protein expression of ERK (Harada et al., 2001; Shah and Lahiri, 2014), the upstream regulator of EGR1. The results showed that the expression of phosphorylated ERK was increased in TS CMs, indicating an elevated ERK activity (Figures 4D and S4K). Previous reports have established a connection between an increased intracellular calcium concentration and ERK activation in CMs (Wheeler-Jones, 2005; Zarain-Herzberg et al., 2011). Therefore, one of the potential mechanisms in TS CMs is that excessive calcium influx through the mutant Ca$_V$1.2 channels causes an increase in ERK activity, resulting in a subsequent induction of EGR1 and an increase in p35 expression. The increased expression of p35 causes CDK5 hyperactivation, which enhances the delayed inactivation of the mutant Ca$_V$1.2 channels, leading to more severe phenotypes in the TS CMs. Thus, CDK5 inhibition using CDK5 inhibitors, DN, or shRNA alleviates the phenotypes in TS CMs (Figure 4E).

DISCUSSION

In this study, we used human CMs derived from the iPSCs generated from the skin fibroblasts of two TS patients to identify additional potential therapeutic compounds based on roscovitine, our previously reported lead compound for TS (Song et al., 2015; Yazawa et al., 2011). We tested the hypothesis that the beneficial effects of roscovitine on TS CMs are associated with its inhibitory effect on CDKs. We revealed a role of CDK5 in the pathogenesis of TS and a mechanism underlying the therapeutic effects of roscovitine on

TS CMs, whereby roscovitine exhibits its effects in part by inhibiting CDK5. Roscovitine has been reported to enhance the voltage-dependent inactivation of $Ca_V1.2$ with the TS mutation in a heterologous overexpression system (Yarotskyy and Elmslie, 2007; Yarotskyy et al., 2009, 2010). Compared with the heterologous system, using TS CMs derived from iPSCs allowed us to examine the effects of roscovitine in a more physiologically relevant cardiac environment. Patient-specific iPSCs provided us with the opportunity to identify key mediators such as CDK5, which is involved in the regulation of $Ca_V1.2$ channels in CMs. Although there are several recent updates that provide insights into the structural and functional changes in the $Ca_V1.2$ channels caused by the TS mutations (Dick et al., 2016; Li et al., 2016) and a few previous reports indicating the potential regulation of $Ca_V1.2$ by CDK5 in pancreatic β cells and a neuronal progenitor cell line (Furusawa et al., 2014; Wei et al., 2005), our findings demonstrate that CDK5 plays an important role in regulating $Ca_V1.2$ functions in CMs and that the inhibition of CDK5 is beneficial for TS CMs.

There are still some concerns in the studies using human iPSC-based disease models, one of which is that patient-specific iPSC-based models of long-QT syndrome demonstrate relatively prolonged action potentials (Itzhaki et al., 2011) relative to the patients' QT intervals. Thus, the iPSC-derived CMs do not fully respond to physiologically relevant high pacing frequencies (1–2 Hz) in calcium imaging and action potential recordings. Another concern is that there might be a progression in the disease phenotypes in iPSC-based models of long-QT syndrome over time, and it would be difficult to identify the optimal time points to examine the effects of therapeutic candidates in the patient-specific CMs (See Supplemental Note).

Although we found the role of CDK5 in cardiac calcium channel regulation, exactly how CDK5 regulates $Ca_V1.2$ channels via phosphorylation in the II-III loop and C-term remains unclear. Therefore, further investigation is necessary to elucidate the molecular mechanisms by which CDK5 phosphorylates and regulates $Ca_V1.2$ channels in CMs. Moreover, based on the consensus sequences targeted by CDK5, CDK5 may have effects on the functions of other ion channels such as HCN4 and Nav1.5, which play important roles in cardiac function. This report provides insights into the molecular bases of cardiac calcium channel regulation and the development of future therapeutics for TS patients.

EXPERIMENTAL PROCEDURES

In brief, human iPSCs were cultured using a standard feeder-free protocol with Essential 8 medium and Geltrex (Thermo-Fisher/Life Technologies) following the manufacturer's instructions. Human control and patient iPSC lines were differentiated into CMs using the monolayer-based in vitro differentiation protocol (Song et al., 2015). Whole-cell patch-clamp recordings in single CM were conducted using standard methods with voltage and current-clamp modes for measuring L-type Ca^{2+}/Ba^{2+} currents and action potentials, respectively. The statistics used for every figure are indicated in the corresponding figure legends. Student's t test (paired or unpaired, two tailed) was conducted with the t test functions in Microsoft Excel software. One-way ANOVA with Bonferroni's or Dunnett's post hoc analyses for multiple comparisons was conducted with the GraphPad Prism software. All data meet the assumptions of the statistical tests. All samples used in this study were biological repeats, not technical repeats. We did not exclude any samples and results from the analyses in this study.

Additional experimental procedures and detailed methodology are described in Supplemental Experimental Procedures.

SUPPLEMENTAL INFORMATION

Supplemental Information includes Supplemental Experimental Procedures, Supplemental Note, four figures, three tables, and one movie and can be found with this article online at http://dx.doi.org/10.1016/j.stemcr.2017.05.028.

AUTHOR CONTRIBUTIONS

L.S. and M.Y. conceived of and designed the project, and analyzed all the data. L.S., S.E.P., Y.I., K.M., and M.Y. performed the experiments. L.S. and M.Y. wrote the manuscript. S.E.P., Y.I., and K.M. edited and proof-read the manuscript. All co-authors approved the submitted manuscript.

ACKNOWLEDGMENTS

We thank A.K. Rinderspacher for providing the chemical information of the Roscovitine analogs; and G. Pitt, R.S. Kass, R. Robinson, H. Colecraft, and S. Marx for helpful discussions. The flow cytometry experiment was performed in the CCTI Flow Cytometry Core at Columbia University, supported in part by the Office of the Director, NIH under awards S10OD020056. Financial support was provided by the Leona M. and Harry B. Helmsley Charitable Trust stem cell starter grant, NIH Pathway to Independent Award (R00HL11345), and startup funds from the Columbia Stem Cell Initiative and Department of Rehabilitation and Regenerative Medicine to M.Y. and the NIH Kirschstein-NRSA predoctoral fellowship (5F31HL131087) award to L.S.

Received: July 14, 2016
Revised: May 22, 2017
Accepted: May 23, 2017
Published: June 22, 2017

REFERENCES

Asada, A., Saito, T., and Hisanaga, S. (2012). Phosphorylation of p35 and p39 by Cdk5 determines the subcellular location of the holokinase in a phosphorylation-site-specific manner. J. Cell Sci. *125*, 3421–3429.

Bettayeb, K., Oumata, N., Echalier, A., Ferandin, Y., Endicott, J.A., Galons, H., and Meijer, L. (2008). CR8, a potent and selective, roscovitine-derived inhibitor of cyclin-dependent kinases. Oncogene *27*, 5797–5807.

Boczek, N.J., Miller, E.M., Ye, D., Nesterenko, V.V., Tester, D.J., Antzelevitch, C., Czosek, R.J., Ackerman, M.J., and Ware, S.M. (2015). Novel Timothy syndrome mutation leading to increase in CACNA1C window current. Heart Rhythm *12*, 211–219.

Brasca, M.G., Albanese, C., Alzani, R., Amici, R., Avanzi, N., Ballinari, D., Bischoff, J., Borghi, D., Casale, E., Croci, V., et al. (2010). Optimization of 6,6-dimethyl pyrrolo[3,4-c]pyrazoles: identification of PHA-793887, a potent CDK inhibitor suitable for intravenous dosing. Bioorg. Med. Chem. *18*, 1844–1853.

Corona-Rivera, J.R., Barrios-Prieto, E., Nieto-Garcia, R., Bloise, R., Priori, S., Napolitano, C., Bobadilla-Morales, L., Corona-Rivera, A., Zapata-Aldana, E., Pena-Padilla, C., et al. (2015). Unusual retrospective prenatal findings in a male newborn with Timothy syndrome type 1. Eur. J. Med. Genet. *58*, 332–335.

Dhariwala, F.A., and Rajadhyaksha, M.S. (2008). An unusual member of the Cdk family: Cdk5. Cell. Mol. Neurobiol. *28*, 351–369.

Dick, I.E., Joshi-Mukherjee, R., Yang, W., and Yue, D.T. (2016). Arrhythmogenesis in Timothy syndrome is associated with defects in Ca(2+)-dependent inactivation. Nat. Commun. *7*, 10370.

Flucher, B.E., and Franzini-Armstrong, C. (1996). Formation of junctions involved in excitation-contraction coupling in skeletal and cardiac muscle. Proc. Natl. Acad. Sci. USA *93*, 8101–8106.

Furusawa, K., Asada, A., Saito, T., and Hisanaga, S. (2014). The effect of cyclin-dependent kinase 5 on voltage-dependent calcium channels in PC12 cells varies according to channel type and cell differentiation state. J. Neurochem. *130*, 498–506.

Harada, T., Morooka, T., Ogawa, S., and Nishida, E. (2001). ERK induces p35, a neuron-specific activator of Cdk5, through induction of Egr1. Nat. Cell Biol. *3*, 453–459.

Hennessey, J.A., Boczek, N.J., Jiang, Y.H., Miller, J.D., Patrick, W., Pfeiffer, R., Sutphin, B.S., Tester, D.J., Barajas-Martinez, H., Ackerman, M.J., et al. (2014). A CACNA1C variant associated with reduced voltage-dependent inactivation, increased CaV1.2 channel window current, and arrhythmogenesis. PLoS One *9*, e106982.

Huebsch, N., Loskill, P., Mandegar, M.A., Marks, N.C., Sheehan, A.S., Ma, Z., Mathur, A., Nguyen, T.N., Yoo, J.C., Judge, L.M., et al. (2015). Automated video-based analysis of contractility and calcium flux in human-induced pluripotent stem cell-derived cardiomyocytes cultured over different spatial scales. Tissue Eng. Part C Methods *21*, 467–479.

Itzhaki, I., Maizels, L., Huber, I., Zwi-Dantsis, L., Caspi, O., Winterstern, A., Feldman, O., Gepstein, A., Arbel, G., Hammerman, H., et al. (2011). Modelling the long QT syndrome with induced pluripotent stem cells. Nature *471*, 225–229.

Jacobs, A., Knight, B.P., McDonald, K.T., and Burke, M.C. (2006). Verapamil decreases ventricular tachyarrhythmias in a patient with Timothy syndrome (LQT8). Heart Rhythm *3*, 967–970.

Kawaida, M., Abe, T., Nakanishi, T., Miyahara, Y., Yamagishi, H., Sakamoto, M., and Yamada, T. (2016). A case of Timothy syndrome with adrenal medullary dystrophy. Pathol. Int. *66*, 587–592.

Li, B., Tadross, M.R., and Tsien, R.W. (2016). Sequential ionic and conformational signaling by calcium channels drives neuronal gene expression. Science *351*, 863–867.

Meijer, L., Borgne, A., Mulner, O., Chong, J.P., Blow, J.J., Inagaki, N., Inagaki, M., Delcros, J.G., and Moulinoux, J.P. (1997). Biochemical and cellular effects of roscovitine, a potent and selective inhibitor of the cyclin-dependent kinases cdc2, cdk2 and cdk5. Eur. J. Biochem. *243*, 527–536.

Oumata, N., Bettayeb, K., Ferandin, Y., Demange, L., Lopez-Giral, A., Goddard, M.L., Myrianthopoulos, V., Mikros, E., Flajolet, M., Greengard, P., et al. (2008). Roscovitine-derived, dual-specificity inhibitors of cyclin-dependent kinases and casein kinases 1. J. Med. Chem. *51*, 5229–5242.

Papineau, S.D., and Wilson, S. (2014). Dentition abnormalities in a Timothy syndrome patient with a novel genetic mutation: a case report. Pediatr. Dent. *36*, 245–249.

Pasca, S.P., Portmann, T., Voineagu, I., Yazawa, M., Shcheglovitov, A., Pasca, A.M., Cord, B., Palmer, T.D., Chikahisa, S., Nishino, S., et al. (2011). Using iPSC-derived neurons to uncover cellular phenotypes associated with Timothy syndrome. Nat. Med. *17*, 1657–1662.

Philipp, L.R., and Rodriguez, F.H., 3rd. (2016). Cardiac arrest refractory to standard intervention in atypical Timothy syndrome (LQT8 type 2). Proc. (Bayl. Univ. Med. Cent.) *29*, 160–162.

Plattner, F., Hernandez, A., Kistler, T.M., Pozo, K., Zhong, P., Yuen, E.Y., Tan, C., Hawasli, A.H., Cooke, S.F., Nishi, A., et al. (2014). Memory enhancement by targeting Cdk5 regulation of NR2B. Neuron *81*, 1070–1083.

Seisenberger, C., Specht, V., Welling, A., Platzer, J., Pfeifer, A., Kuhbandner, S., Striessnig, J., Klugbauer, N., Feil, R., and Hofmann, F. (2000). Functional embryonic cardiomyocytes after disruption of the L-type alpha1C (Cav1.2) calcium channel gene in the mouse. J. Biol. Chem. *275*, 39193–39199.

Shah, K., and Lahiri, D.K. (2014). Cdk5 activity in the brain—multiple paths of regulation. J. Cell Sci. *127*, 2391–2400.

Shah, D.P., Baez-Escudero, J.L., Weisberg, I.L., Beshai, J.F., and Burke, M.C. (2012). Ranolazine safely decreases ventricular and atrial fibrillation in Timothy syndrome (LQT8). Pacing Clin. Electrophysiol. *35*, e62–e64.

Song, L., Awari, D.W., Han, E.Y., Uche-Anya, E., Park, S.H., Yabe, Y.A., Chung, W.K., and Yazawa, M. (2015). Dual optical recordings for action potentials and calcium handling in induced pluripotent stem cell models of cardiac arrhythmias using genetically encoded fluorescent indicators. Stem Cells Transl. Med. *4*, 468–475.

Splawski, I., Timothy, K.W., Sharpe, L.M., Decher, N., Kumar, P., Bloise, R., Napolitano, C., Schwartz, P.J., Joseph, R.M., Condouris, K., et al. (2004). Ca(V)1.2 calcium channel dysfunction causes a multisystem disorder including arrhythmia and autism. Cell *119*, 19–31.

Wei, F.Y., Nagashima, K., Ohshima, T., Saheki, Y., Lu, Y.F., Matsushita, M., Yamada, Y., Mikoshiba, K., Seino, Y., Matsui, H., et al. (2005). Cdk5-dependent regulation of glucose-stimulated insulin secretion. Nat. Med. *11*, 1104–1108.

Wheeler-Jones, C.P. (2005). Cell signalling in the cardiovascular system: an overview. Heart *91*, 1366–1374.

Yarotskyy, V., and Elmslie, K.S. (2007). Roscovitine, a cyclin-dependent kinase inhibitor, affects several gating mechanisms to inhibit cardiac L-type (Ca(V)1.2) calcium channels. Br. J. Pharmacol. *152*, 386–395.

Yarotskyy, V., Gao, G., Peterson, B.Z., and Elmslie, K.S. (2009). The Timothy syndrome mutation of cardiac CaV1.2 (L-type) channels: multiple altered gating mechanisms and pharmacological restoration of inactivation. J. Physiol. *587*, 551–565.

Yarotskyy, V., Gao, G., Du, L., Ganapathi, S.B., Peterson, B.Z., and Elmslie, K.S. (2010). Roscovitine binds to novel L-channel (CaV1.2) sites that separately affect activation and inactivation. J. Biol. Chem. *285*, 43–53.

Yazawa, M., Hsueh, B., Jia, X., Pasca, A.M., Bernstein, J.A., Hallmayer, J., and Dolmetsch, R.E. (2011). Using induced pluripotent stem cells to investigate cardiac phenotypes in Timothy syndrome. Nature *471*, 230–234.

Zarain-Herzberg, A., Fragoso-Medina, J., and Estrada-Aviles, R. (2011). Calcium-regulated transcriptional pathways in the normal and pathologic heart. IUBMB Life *63*, 847–855.